Table 3 Test case I, "regular" Athena; results using bilinear equations[a]

Run	Ballistic wind, m/sec	Iteration to impact: θ_{1L}, rad	θ_{2L}, rad	X, km	Y, km	To burnout angles: θ_{1L}, rad	θ_{2L}, rad	θ_{2b}, rad	θ_{2b}, rad
Nominal		−0.2121	0.1151	306.2	−643.7	−0.2121	0.1151	−0.6597	0.3753
1	−4.15	−0.1470(68)	0.1480(79)	304.8(.6)	−643.7(.5)	−0.1456(49)	0.1477(2)	−0.6640(20)	0.3762(45)
	−8.93	−0.1472(3)	0.1486(83)	306.1(.2)	−643.7	−0.1441	0.1476	−0.6599(8)	0.3754(3)
2	−12.91	−0.2473(81)	0.2133(5)	299.9	−646.0(7.1)	−0.2493(0)	0.2147(5)	−0.6642(35)	0.3666(57)
	5.11	−0.2467	0.2155	306.6	−643.7(.8)	−0.2474(5)	0.2175(6)	−0.6598	0.3758
		−0.2466	0.2153	306.1	−643.7				
3	−11.29	−0.2871(81)	0.2002(11)	303.6(5.2)	−643.1(4.1)	−0.2901(896)	0.2019(23)	−0.6631(17)	0.3748(55)
	10.59	−0.2879	0.2014	306.2	−643.7	−0.2889	0.2022	−0.6596(97)	0.3753
4	2.55	−0.1376(7)	0.0969(72)	304.7(5.6)	−643.1(2.9)	−0.1354(47)	0.0959	−0.6658(41)	0.3779
	−10.36	−0.1383(4)	0.0976	306.2(.1)	−643.7(.6)	−0.1333(2)	0.0953	−0.6600(599)	0.3754
5	−3.66	−0.2600(2)	0.1423(5)	305.3(.8)	−644.2(.3)	−0.2616(4)	0.1431(2)	−0.6580(95)	0.3720(3)
	6.71	−0.2598	0.1426	306.2	−643.7(.6)	−0.2622	0.1441(0)	−0.6598	0.3753
6	8.10	−0.2311(2)	0.0528(5)	307.6(6.5)	−641.5(.8)	−0.2310(07)	0.0523(19)	−0.6599(0)	0.3786(70)
	2.48	−0.2325	0.0527(8)	306.2	−643.6(.7)	−0.2310	0.0513	−0.6597(8)	0.3752(3)

[a] Numbers in parentheses indicate the changes in the last one or two figures when the quadratic equations are used; e. g., in Run 1*a*, first iteration, $\theta_{1L} = -0.1468$ and $Y = -643.5$ if quadratic equations are used.

ponents of ballistic wind, W_x, W_y. An examination of the residuals indicated that both forms provided a good fit to the data.

Evaluation of the Procedure

Sixteen different wind profiles were used to evaluate the foregoing equations. Six of them are shown in Fig. 2. Some of these profiles were measured during missile support operations at White Sands Missile Range while the others are hypothetical. Four rockets were used in the evaluation: two configurations of the Athena which have quite different nominal trajectories; the Aerobee-350; and the Ballistic Missile Target System (BMTS).

Two independent iterations were performed. The first was to match nominal impact; the second was to match nominal burnout angles. A convergence tolerance of 1500 m was selected for the impact iteration except for one case, the "regular" Athena where a tolerance of 300 m was used. This smaller tolerance was used to show the speed with which the iteration converges. Compatible tolerances, which differed for each rocket, were used for the iterations to burnout angles.

The first and most exhaustive test was performed on the "regular" Athena. This is a typical configuration of several slightly different Athena missiles fired from Green River, Utah, to impact on White Sands Missile Range. The Athena is a two-stage (for the ascent trajectory) unguided rocket which is fired at a nominal elevation angle of ~13.5° and achieves an apogee of ~250 km and a range of 725 km.

Both the quadratic and bilinear equations were used to perform the iterations; these were performed as independent cases. The results (for the 6 profiles shown in Fig. 2) are presented in Table 3. Two things should be observed: both expressions provide rapid convergence, and there is no significant difference in the results obtained from the two expressions. This suggests the use of the simpler bilinear equations. The results from the other test cases (3 other missiles and 10 other wind profiles) were quite similar and will not be presented here.

References

[1] Lewis, J., "The Effect of Wind and Rotation of the Earth on Unguided Rockets," Rept. 685, March 1949, Ballistic Research Lab., Aberdeen Proving Ground, Md.

[2] James, R. and Harris, R., "Computation of Wind Compensation for Launching of Unguided Rockets," TN D-465, Nov. 1960, NASA.

[3] Hennigh, K., "Field Wind Weighting and Impact Prediction for Unguided Rockets," TN D-2142, March 1964, NASA.

[4] Duncan, L. and Engebos, B., "Techniques for Computing Launcher Settings for Unguided Rockets," ECOM 5077, Sept. 1966, and "A Nomogram for Field Determination of Launcher Settings for Unguided Rockets," ECOM 5088, Oct. 1966, Atmospheric Sciences Lab., White Sands Missile Range, N. Mex.

[5] Duncan, L. and Rachele, H., "Real Time Meteorological System for Firing of Unguided Rockets," *Journal of Applied Meteorology*, Vol. 6, No. 2, April 1967, pp. 396–400.

An Advanced Laser Tracking Technique for Future Space Guidance Systems

CHARLES L. WYMAN*
NASA Marshall Space Flight Center, Ala.

Nomenclature

t = time to scan total field
Φ,Ψ = total and instantaneous fields of view
K = overlap ratio
R = maximum range
c = velocity of light
τ = signal recognition time

Introduction

MANY space guidance and communication requirements are best solved by use of lasers. In particular, cooperative spacecraft offer a variety of situations in which laser radar and communication techniques are by far the best alternative.[1,2] For simple radar functions, a corner reflector on the target vehicle will greatly enhance system performance. For more complicated situations, angle trackers, acquisition beacons, or complete transceivers may be mounted on the target vehicle to provide various capabilities. A complete transceiver system on each spacecraft allows determination of total radar information on both spacecraft while simultaneously providing a two-way communications capability.

Received August 15, 1969; presented as Paper 69-870 at the AIAA Guidance, Control, and Flight Mechanics Conference, Princeton, N.J., August 18–20, 1969; revision received October 23, 1969.

* Deputy Chief, Applied Physics Branch, Technology Division, Astrionics Laboratory.

Table 1 Laser characteristics

Operating temperature	25°C
Power out	1 w peak
Pulse rate	10 kHz
Wavelength	9050 Å ±50 Å
Pulse width	30–100 nanosec

Laser systems, with the immense antenna gains available at optical frequencies, are simpler, lighter, smaller, and lower in power consumption than other systems. In the past the resultant very narrow beams have had to be accommodated by pointing and tracking with precision gimbals. Now a system is being developed using precision laser beam deflectors[3] which allow the beam to be scanned synchronously with a scanned detector. This advanced tracking technique provides a wide-angle capability without the use of gimbals.

System Concept and Design Basis

Consider an optical tracking system, using image dissectors, raster scanning a small instantaneous field of view Ψ over a larger total field Φ.[4] The raster utilizes stepped triangular waves and provides a scan (Fig. 1). The small instantaneous field dwells momentarily at each position before moving on. If a target appears in any dwell position, it is detected, and the tracker automatically goes into a cross-scan tracking mode. The waveforms and scan pattern for tracking are indicated in Fig. 2. The illustrations are based upon a square Ψ. In the tracking mode, the steps are small compared with Ψ.

Now consider a narrow laser beam with the beam divergence approximately equal to Ψ. If this beam scans synchronously with the tracker and on a common optical axis, any object in the field will be momentarily illuminated as the beam scans across. An object would be detected in the field provided that 1) sufficient energy from the beam is reflected back to the tracker and 2) the beam and Ψ dwell on the target an amount of time exceeding the round trip transit time of light plus the period of time required for signal detection. If a corner reflector is present on the object, the amount of light returned to the tracker is increased several orders of magnitude.

Transit time of the light and relative angular rates between vehicles are the only parameters that are restrictive in designing systems using the advanced tracking technique. Successive beam positions and successive lines must overlap during acquisition to accommodate relative angular rates. The time to scan the total acquisition field is

$$t = \Phi^2 (2R/c + \tau)/\Psi^2(1 - K)^2 \qquad (1)$$

and angular rates may be accommodated up to

$$V = [K(1 - K)\Psi^2/2\Phi(2R/c + \tau)] \qquad (2)$$

If target angular position is known to much less than Φ, then higher V's may be acquired by scanning only the area of uncertainty within Φ. For example, if the target positions were known to within $\Phi/10$, then rates to $10V_{max}$ could be acquired, and the acquisition time would be only $0.01t$. Once acquired, the system will track objects with much greater relative angular rates than can be tolerated during acquisition. Scan patterns may be computer-controlled and can be optimized for specific applications. For exceptional missions higher V's may be acquired by use of an acquisition beacon on the target vehicle.

Table 2 Beam deflector characteristics

Resonant frequency	1250 Hz
Operating bandwidth	0–1 kHz
Spot resolution	300 spots
Deflection linearity	0.1% minimum
Beam deflection	±0.625°
Nominal aperture	1.25 cm

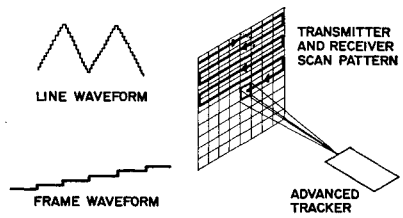

Fig. 1 Raster scan pattern for acquisition.

System Description

The system presently under development is based on the configuration shown in Fig. 3, and it will be tested with and without the optional acquisition beacon and target vehicle angle tracker. It may acquire either by having the chaser vehicle tracker search for the acquisition beacon or by scanning the laser beam synchronously with the tracker Ψ until the corner reflector is encountered. Once acquired, the target tracker sees the beam from the chaser and tracks it, while the chaser vehicle tracks the reflected beam. If there is a change in the relative angular position, the laser beam and tracker Ψ synchronously move to continue illuminating the target. Tracking is accomplished anywhere within Φ.

This particular system utilizes square Φ of 30° × 30°, with Ψ of 0.1° × 0.1°. The laser[5] is a single-mode, diffraction-limited, pulsed GaAs device and puts out a circular beam approximately 0.1° × 0.1°. The laser characteristics are summarized in Table 1.

The optical layout for the laser transmitter-beam deflector system is depicted in Fig. 4. The beam deflectors accept a 1.25-cm-diam diffraction-limited beam and deflect it over ±0.625° = ±2250 arcsec. The half-power divergence angle of this beam is $\theta = \lambda/D = 0.9 \times 10^{-4}$ cm/1.25 cm = 72μ rad = 14.8 arcsec. This gives 2(2250 arcsec)/14.8 arcsec = 304 spot positions. The beam diameter is reduced and the divergence is increased (Fig. 4) to accomplish a 0.1° + 0.1° beam deflected over a 30° × 30° field. The nominal characteristics of the beam deflectors[3,6] are summarized in Table 2.

Digital techniques are used throughout the tracker. The system is arranged to raster scan with alternate frames orthogonal to one another with steps of 0.08°; this allows relative angular rates between vehicles to be greater during acquisition than can be allowed by scanning in one direction only. It also is set up to scan either at one frame each 140.6 sec or at one frame each 14.06 sec. The former gives a dwell time of 1 msec, allowing acquisition out to 150 km, with tracking rates up to 1.25°/sec. At close ranges the system is switched to fast scan, where rates to 12.5°/sec may be followed. It also has a rapid reacquisition capability; in this mode, if tracking is lost momentarily, the system goes into a limited acquisition scan. Four frames encompassing a 1.28° × 1.28° field are scanned after track loss. If reacquisition does not occur after four frames, the system goes back to the full 30° × 30° acquisition mode.

Some salient features of the operation of the electronics follow. A tracker clock pulse controls the rate of operation

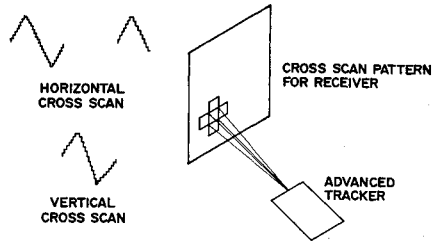

Fig. 2 Cross scan pattern for tracking.

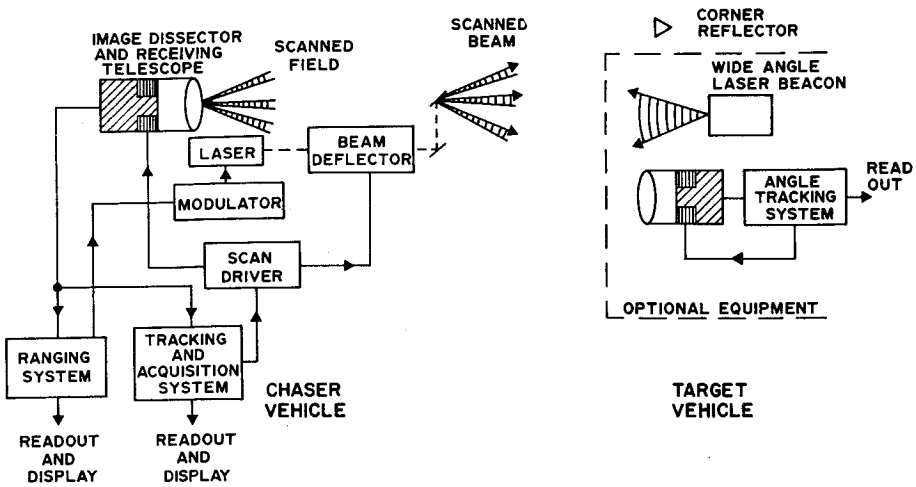

Fig. 3 Basic advanced tracking system.

and determines whether the system operates in the fast or the slow scan mode. The laser beam and image dissector are scanned synchronously. When the corner reflector is encountered in the field of view, a return pulse operates on the acquisition-track mode control and causes the scanning to stop for an additional dwell time. If the corner reflector actually is in the field, a second pulse will be detected to affirm acquisition. The mode control then causes the system

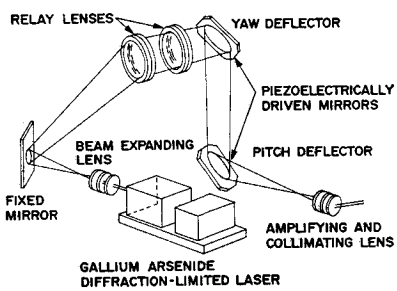

Fig. 4 Advanced tracking technique transmitter optics.

to begin tracking by turning off the acquisition counter and turning on a tracking counter. The track counter digital-to-analog converter is scaled to give track scan steps $\frac{1}{8}$ the size of the acquisition scan step (0.01°).

The received signal pulses are processed digitally to obtain angular position and angular velocity. The position counter is reset to its center position after each cross scan. If the target is centered, equal numbers of pulses are received during positive and negative excursions of the cross scan, and the reset causes no counter output. If the target is off center, more pulses are received during one excursion than the other, and the position counter ends up off center. Resetting causes a counter output proportional to the position error. The system requires a transmitter pulse rate of at least one pulse per dwell time. At this pulse rate the angular position resolution corresponds to $\pm\frac{1}{4}$ track scan step ($\pm 0.0025°$). A minimum accuracy of $\pm 0.01°$ is obtained throughout Φ.

Velocity is treated similarly to position, except that the counter is not reset; its center position corresponds to $V = 0$. If it ends up off center, the difference is proportional to V and may be used to correct position errors caused by the relative angular velocity.

The receiver objective is an f 0.95, 50-mm, wide-angle lens. This focal length corresponds to an image dissector instantaneous aperture size of 88.9 μ to obtain Ψ of 0.1°. The image dissector is an F4011 with an S1 cathode with special ultralinear deflection coils. The Ψ of 0.1° and the 0.08° raster scan steps provide a 20% overlap. With this overlap and with alternate frames scanning orthogonally, the slow scan rate will accommodate V's during acquisition of

$$\frac{(1 - 0.2)[0.2(1 - 0.2)(0.1)^2]}{0.2 \times 2 \times 30 \times 10^{-3}} = 0.1064°/\text{sec}$$

according to Eq. (2). This rate is sufficient for nominal rendezvous trajectories. For exceptional missions an additional acquisition beacon may be required.

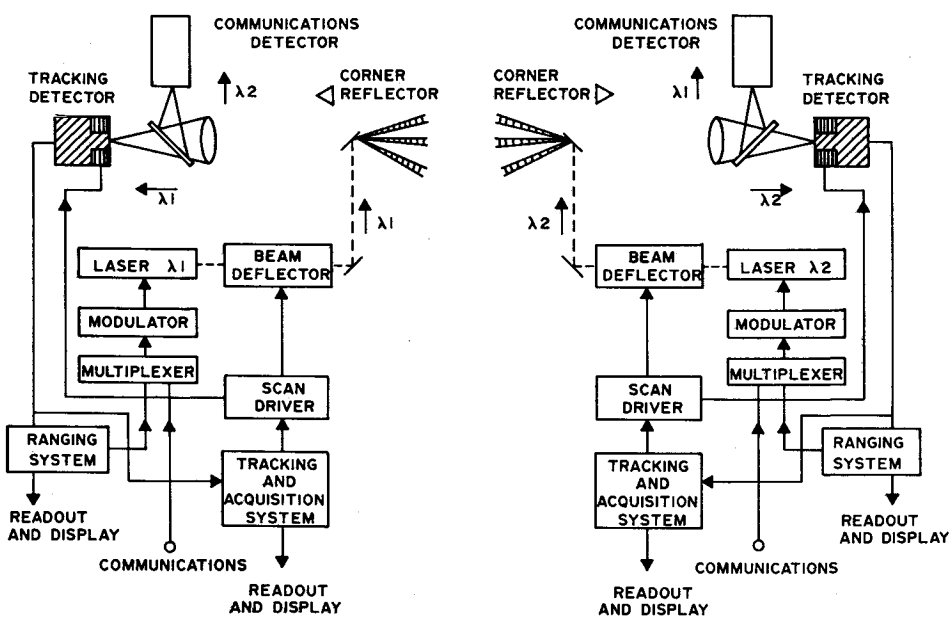

Fig. 5 Multisystem laser tracker.

Applications

The specific equipment now being fabricated (Fig. 3) is tailored to rendezvous and docking applications. With the optional target vehicle angle tracker and acquisition beacon, it will suffice for nearly all conceivable cooperative rendezvous and docking situations. It will operate automatically or will provide display information. Range rate may be easily measured to the accuracies necessary to provide automatic docking of large vehicles, a function that apparently cannot be satisfied easily by other techniques.

For certain limited applications, rendezvous may be accomplished without the optional equipment. However, for docking, the relative angular position of the target vehicle must still be known. An astronaut on board the chaser vehicle can supply this information visually, and docking can be accomplished, provided that the chaser vehicle can move laterally to obtain angular alignment. This information could also be obtained from the target vehicle via a communications link. The instrument for measuring angular position in this case would be a very small telescope focusing onto a solid-state quadrant detector.

Figure 5 shows a system that has a complete transceiver at either terminal. Two transmitters operate at slightly different wavelengths to separate radar and communication functions. The two wavelengths are separated by dichroic beamsplitters in each transceiver as indicated and directed to radar and communications detectors. The communications capability could also be provided by a physically separate receiver. Since the telescopes are so small, no great penalty would be involved.

Such a system may be applied to a variety of situations. For instance, some astronomical payloads are required to be unmanned for stability and contamination considerations. At the same time the vehicle must be controlled and monitored during acquisition and observation of astronomical objects, and also administered occasionally for maintenance or for removal and replacement of photographic supplies. Such a payload requires station-keeping by a remote satellite, with a command communication link to it and a monitoring link from the payload. With the system shown in Fig. 5, the radar can be programmed to maintain a certain range between the spacecraft, while for maintenance the payload can be commanded back to the manned satellite. In a similar manner this system can provide a station-keeping and two-way communications capability for an orbital assembly, fueling, and launch facility. Other configurations could provide a) rendezvous and docking automatically for supply shuttles to space stations or for space rescue missions, or b) station-keeping and communications link between stationary atellites and terminals on the moon or earth.

Conclusions

The addition of the wide-angle, gimballess capability of the advanced tracking technique greatly enhances the over-all versatility and performance capacity of laser radars for rendezvous and docking. Even if a particular vehicle or payload requires hemispherical coverage, it can be done with an indexed and mechanically latched gimbal system far simpler and more reliable than with precision gimbals. The wide-angle capability allows wide-angle limit-cycling in rendezvous and station-keeping applications, with a resultant large savings in fuel, and the capability for tracking high angular rates allows vehicle maneuvers to take place simultaneous to tracking.

The versatility of providing radar and communication functions on the same sensor system is a tremendous aid in station-keeping applications. Presently, bandwidths of several tens of kilobits per second can be provided. One megabit with room temperature GaAs lasers is expected within the year, and eventually these devices may be used to transmit real-time television.

Other techniques would require two or even three complete systems to provide rendezvous radar, docking radar, station-keeping, and communications systems capacity. This system is smaller, weighs less, and uses less power than any one of the other systems but can simultaneously provide all of these capabilities to most of these missions.

References

[1] Dixon, T. P., Wyman, C. L., and Coombes, H. D., "A Laser Guidance System for Rendezvous and Docking," *Navigation—The Journal of the Institute of Navigation*, Vol. 13, No. 3, Autumn 1966.

[2] Wyman, C. L., "Test Performance of an Experimental Laser Radar for Rendezvous and Docking," *The Journal of Spacecraft and Rockets*, Vol. 5, No. 4, April 1968, pp. 430–433.

[3] Fowler, V. J. et al., "Investigation of Electro-Optical Techniques for Controlling the Direction of a Laser Beam," Interim Report TR 65-722.8, General Telephone and Electronics Labs., Bayside, N. Y.

[4] Eberhardt, E. H., "Tracking Properties of ITTIL Deflectable Multiplier Phototubes," Applications Note E-3, Dec. 6, 1963, ITT.

[5] Rutz, E. M., and Edmonds, H. D., "Diffraction Limited Gallium Arsenide Laser," Final Report, FSC 68 0718/4596, Oct. 15, 1968, IBM, Gaithersburg, Md.

[6] Fowler, V. J. et al., "Investigation of Electro-Optical Techniques for Controlling the Direction of a Laser Beam," Interim Report TR 66-722.17, General Telephone and Electronics Labs., Bayside, N. Y.

Effects of Simulated Mars Dust Erosion Environment on Thermal Control Coatings

G. L. Adlon* and E. L. Rusert†
McDonnell Douglas Corporation, St. Louis, Mo.
and
W. S. Slemp‡
NASA Langley Research Center, Hampton, Va.

Nomenclature

T_e	= exposure time, min or hr
α_s	= solar absorptance
$\Delta W, \Delta t$	= weight and thickness losses, 10^{-2} g and 10^{-4} in.
ϵ_{tn}	= total normal infrared emittance
$\rho_d^* \equiv \rho_d/\rho_{do}$	= normalized dust density; $\rho_o \equiv 1.0 \times 10^{-4}$ oz/ft^3
θ	= angle between specimen surface and wind vector, deg

Introduction

THE Viking project is expected to land a vehicle on Mars in 1973 to conduct scientific experiments for 90 days. The postulated Martian environment has a solar constant of

Presented as Paper 69-1023 at the AIAA Fourth Space Simulation Conference, Los Angeles, Calif., September 8–10, 1969; submitted September 11, 1969; revision received January 26, 1970. This work was sponsored under a NASA Langley Funded Contract: NAS-1-8708, "Planetary Environment Simulation Experimental Study," Task 3-Erosion and Dust Coating Effects. The authors wish to acknowledge the assistance of T. H. Allen, J. J. Henderson, and C. R. Johnson.

* Senior Engineer, Space Simulation and Systems Laboratories, McDonnell Aircraft Company.

† Senior Engineer, Material and Processes, McDonnell Douglas Astronautics Company—Eastern Division.

‡ Aerospace Technologist, Coating and Surface Section, Chemistry and Physics Branch of the Applied Materials and Physics Division. Member AIAA.